ADVANCED OPTICAL MATERIALS
www.advopticalmat.de

Supramolecular Two-Photon Switch for Near-Infrared (NIR) Cell Imaging

*Jie Yu, Jie Niu, Hui Wang, Cong-Hui Wang, and Yu Liu**

A light controllable two-photon near-infrared (NIR) optical probe is conveniently constructed by multivalent supramolecular co-assembly of amphiphilic sulfonatocalix[4]arene (SC4A), tricationic triphenylamine (TPA), and diarylethene derivative (DE). The obtained results indicate that the formed SC4A/TPA nanoparticle displays assemble-confined behaviors and enhances the two-photon excited NIR emission. Benefiting from the reversible ring-opened and closed behaviors of the DE under 365 and > 600 nm light irradiation, the dicationic DE in the assembly could act as an energy acceptor after 365 nm light irradiation, then the co-assembly of SC4A/TPA/DE could achieve a NIR fluorescence ON and OFF switch and is successfully applied in HeLa cell imaging, providing a convenient approach to supramolecular two-photon switch for cell imaging.

1. Introduction

Multivalent supramolecular assembly of the macrocyclic hosts and the guests with positive or negative charges not only be used as drug carriers to achieve the targeted drug delivery but also loaded with fluorescent or phosphorescent dyes as optical probes for targeted cell imaging.[1] In the study of macrocyclic multivalent supramolecular assembly, including cyclodextrins,[2,3] cucurbiturils[4,5] and calixarenes,[6–8] in which calixarenes have attracted wide attention mainly due to the upper rim of calixarenes easily modified with the positive or negative functional groups and the lower rim of the host could be grafted with hydrophobic alkyl chains to form amphiphilic calixarene.[9–11] Utilizing the inherent advantages of the amphiphilic calixarene mentioned above, which could encapsulate positive or negative guests to form functional supramolecular assembly,[12–14] provides the confined environment for luminophores to give highly efficient fluorescence or phosphorescence emission in aqueous solution. For example, Klymchenko et al. found that the cationic amphiphilic calixarene with alkyne units could self-assemble to form micelles, which further reacted with cyanine bisazides derivatives to give protein-sized bright nanoparticles with 7 nm diameter, showing good imaging contrast in living cells.[15] Hirsch group developed amphiphilic calixarene containing Newkome-type dendrons groups and two pyrene units, which self-assembled via π–π and hydrophilic-hydrophobic interactions to form nano-platelets with near-infrared (NIR) fluorescence at 652 nm in water.[16] Recently, we also found that amphiphilic sulfonatocalix[4]arene could co-assemble with dibromophthalimide derivative/cucurbit[7]uril complexes to further enhance the phosphorescence lifetime of luminophores from 22.0 μs to 1.13 ms, and then loaded energy acceptors to form cascaded phosphorescence light-harvesting system with delayed fluorescence emission at 675 nm, which was further applied in multicolor cell imaging.[17] On the other hand, when the photo-responsive functional blocks were introduced in the assembly to form a light-controllable supramolecular switch, which could regulate fluorescence and phosphorescence in vitro cells.[18] Zhang et al.[18b] constructed photo-controllable fluorescence color-tunable nanoprobe by the assembly of the coumarin-modified spiropyran derivative and the copolymer of MPEG-*b*-PBMA, which could recognize the sulphite after being activated by UV light, giving constant blue fluorescence, and was further applied in photochromic imaging and sulphite detection in lysosomes. In recent research, we presented a linear supramolecular assembly based on anthracene-modified bromophenylpyridinium salt and cucurbit[8]uril, which showed the photooxidation-driven from red fluorescence to strong green phosphorescence emission, and also acted as a dual organelle-targeted probe for nuclei and lysosomes in living cells after the photochemical reaction.[19] Kim et al. demonstrated that by the energy transfer switchable strategy, diarylethene derivative and Cy5.5 dyes modified dendritic nanoclusters could realize high-contrast NIR luminescence photo-switching in single photon cell imaging.[20a] However, the light-controllable two-photon excited NIR luminescence supramolecular assembly based on the multivalent assembly of amphiphilic calixarene in vitro cell imaging is rarely reported to the best of our knowledge.

In the present research, we reported the assemble-confinement enhanced guest molecule NIR luminescence by the multivalent supramolecular assembly of sulfonatocalix[4]arene (SC4A), tricationic triphenylamine (TPA), and diarylethene derivative (DE), in which the guest TPA with three pyridyl cations and tripaddle rigid structure is easy to interact with amphiphilic calixarene to form supramolecular assembly, which not only benefits to the enhancement of NIR fluorescence

J. Yu, J. Niu, H. Wang, C.-H. Wang, Y. Liu
College of Chemistry
State Key Laboratory of Elemento-Organic Chemistry
Nankai University
Tianjin 300071, P. R. China
E-mail: yuliu@nankai.edu.cn

The ORCID identification number(s) for the author(s) of this article can be found under https://doi.org/10.1002/adom.202301473

DOI: 10.1002/adom.202301473

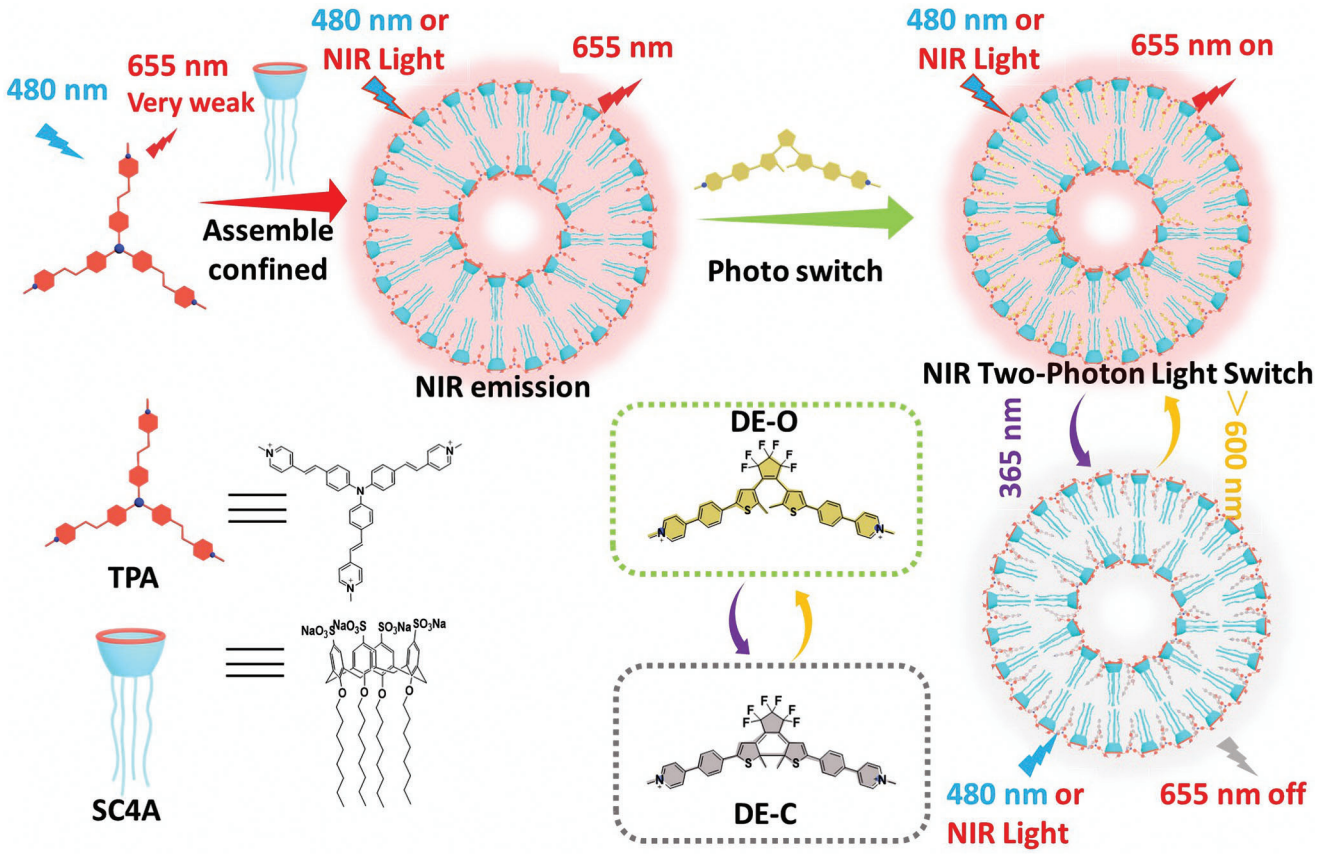

Scheme 1. Light-controllable two-photon NIR fluorescence supramolecular assembly based on amphiphilic calix[4]arene.

emission at 655 nm but also shows two-photon absorption effect. Especially, the co-assembly containing the dicationic photo-switch DE exhibited light-controllable two-photon NIR luminescence and was successfully applied in vitro cell imaging (**Scheme 1**).

2. Results and Discussion

First, the guest-tricationic triphenylamine derivative was synthesized and confirmed by nuclear magnetic resonance (NMR) and mass spectrometry experiments (Figures S1–S3, Supporting Information). Although the guest alone exhibited negligible fluorescence emission in water (Figure S4, Supporting Information), TPA may give good luminescence properties under the confinement of macrocyclic compounds. Subsequently, we studied the binding behavior between SC4A and TPA by the UV–vis spectrometer. As can be seen from Figure S5 (Supporting Information), the absorption signal of the guest-TPA exhibited decreasing trend upon the addition of SC4A, and its maximum absorption peak was shifted from 470 to 480 nm, which may be attributed to the formation of the supramolecular complex with enhancing ICT from the phenyl group to pyridinium units. The assemble behavior between the host and TPA was also investigated by the transmittance experiments, and the signal changes at 700 nm were selected for transmittance analysis to avoid the influence of UV–vis absorption of guest on the transmittance of the system. In Figures S6–S9 (Supporting Information), the transmittance of the host and guest at 700 nm has no apparent change in 10–30 μM, indicating neither SC4A nor TPA could cluster to form large aggregates. With the addition of TPA, the optical transmittance of SC4A (fixed at 10 μM) at 700 nm was obviously decreased (**Figure 1**a), and the calculated critical aggregation concentration (CAC) of TPA was 6.5 μM (Figure 1b), indicating amphiphilic SC4A could effectively reduce the CAC of the guest and induce TPA to form large aggregates. Subsequently, the best binding ratio between SC4A and guest was also studied. As shown in Figure 1c, when the different mounts of the host were added into TPA (fixed at 10 μM), the transmittance of the system gradually decreased and reached the minimum value at 7.5 μM, indicating the best binding ratio between TPA and SC4A was 1:0.75 (Figure 1d).[21,22]

The morphology and size of the supramolecular assembly of SC4A-confined guest were also studied by transmission electron microscope (TEM) and scanning electron microscope (SEM). Many nanoparticles with 20–80 nm diameters were found in TEM picture (**Figure 2**a). In SEM test, spherical nanoparticles are also observed in Figure 2b, which further confirmed that the SC4A/TPA self-assembled to form assemblies. Meanwhile, the dynamic light scattering (DLS) test showed that the average hydrodynamic diameter of the SC4A/TPA was 57 nm (Figure S10, Supporting Information), consistent with TEM and SEM tests. Based on the study of the morphology and size of the

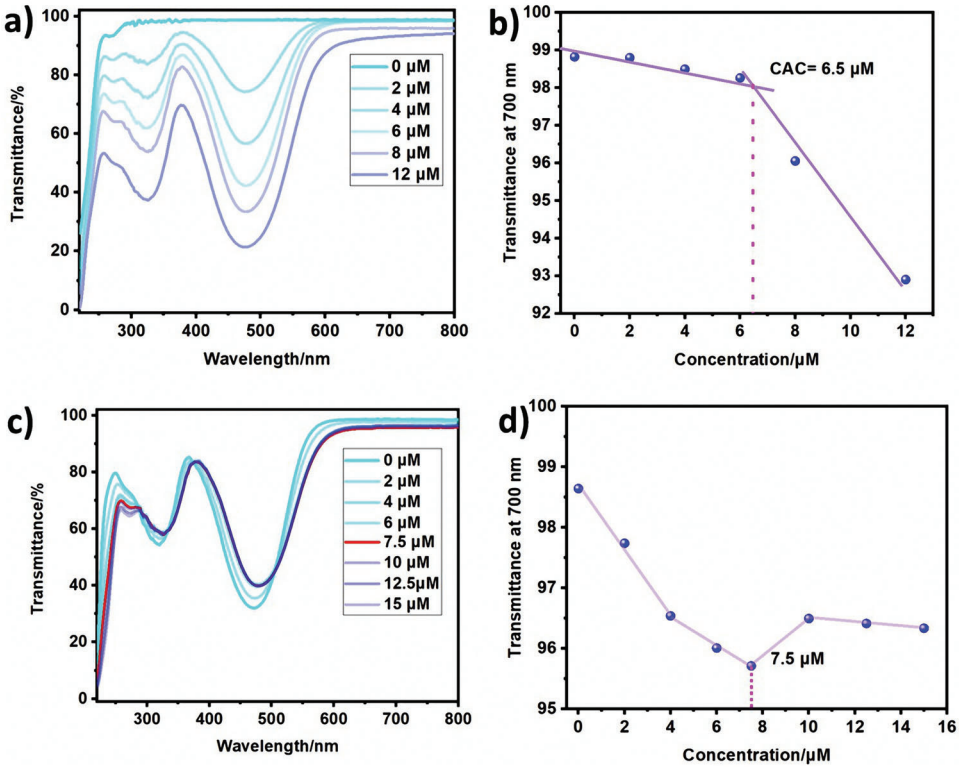

Figure 1. a) The optical transmittance spectra of SC4A in the presence of different mounts of TPA ([SC4A] = 10 μM). b) The optical transmittance of SC4A at 700 nm with the addition of different mounts of TPA ([SC4A] = 10 μM). c) The optical transmittance spectra of TPA in the presence of different mounts of SC4A ([TPA] = 10 μM). d) The optical transmittance of TPA at 700 nm with the addition of different mounts of SC4A ([TPA] = 10 μM).

supramolecular assembly, it is reasonable to speculate that SC4A could bind guests to form a compact structure and further assemble to form ordered and stable nanoparticles (Scheme 1).

Next, we also investigated the binding behavior between SC4A and guest by fluorescence and NMR experiments. In Figure S11 (Supporting Information), the Job experiment result manifested that SC4A could bind with TPA to form a 1:1 type complex. According to the fluorescence intensity changes of TPA at 655 nm (Figure S12, Supporting Information), the binding constant between SC4A and guest was measured to be 3.17×10^7 M^{-1}, which indicated that SC4A could bind TPA by strong non-covalent interaction and then benefit from forming stable complexes. As shown in ^{1}H NMR experiments (Figure S13, Supporting Information), the protons ($H_{a,b,c}$) of TPA were broadened and shifted slightly in the presence of SC4A, and the proton peaks of the SC4A cavity gave less upfield shift compared with the alkyl groups of SC4A, manifesting the guest molecule was not encapsulated by the cavity of SC4A. Thus, the formation of the SC4A/TPA complex may be mainly driven by electrostatic interaction and then further assembled by hydrophobic interaction to form the supramolecular assembly.[22b] Subsequently, fluorescence experiments were also applied to investigate the luminescence behavior of TPA under the confinement of SC4A. As can be seen from **Figure 3**a, the fluorescence intensity of TPA was

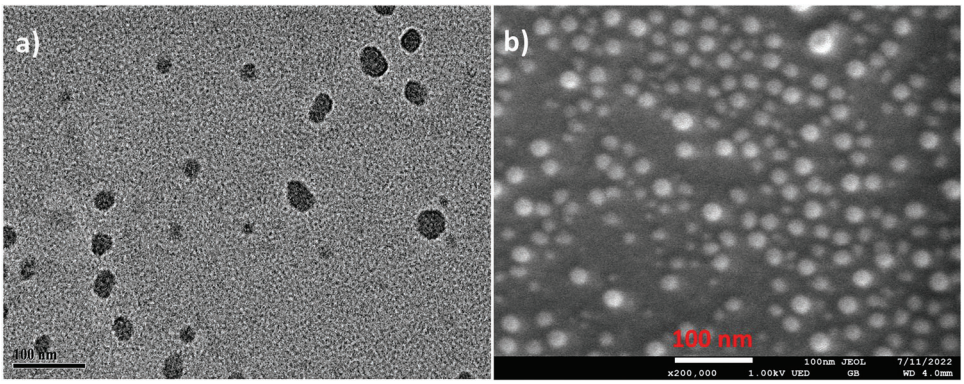

Figure 2. a) TEM image of SC4A/TPA assembly. b) SEM image of SC4A/TPA assembly.

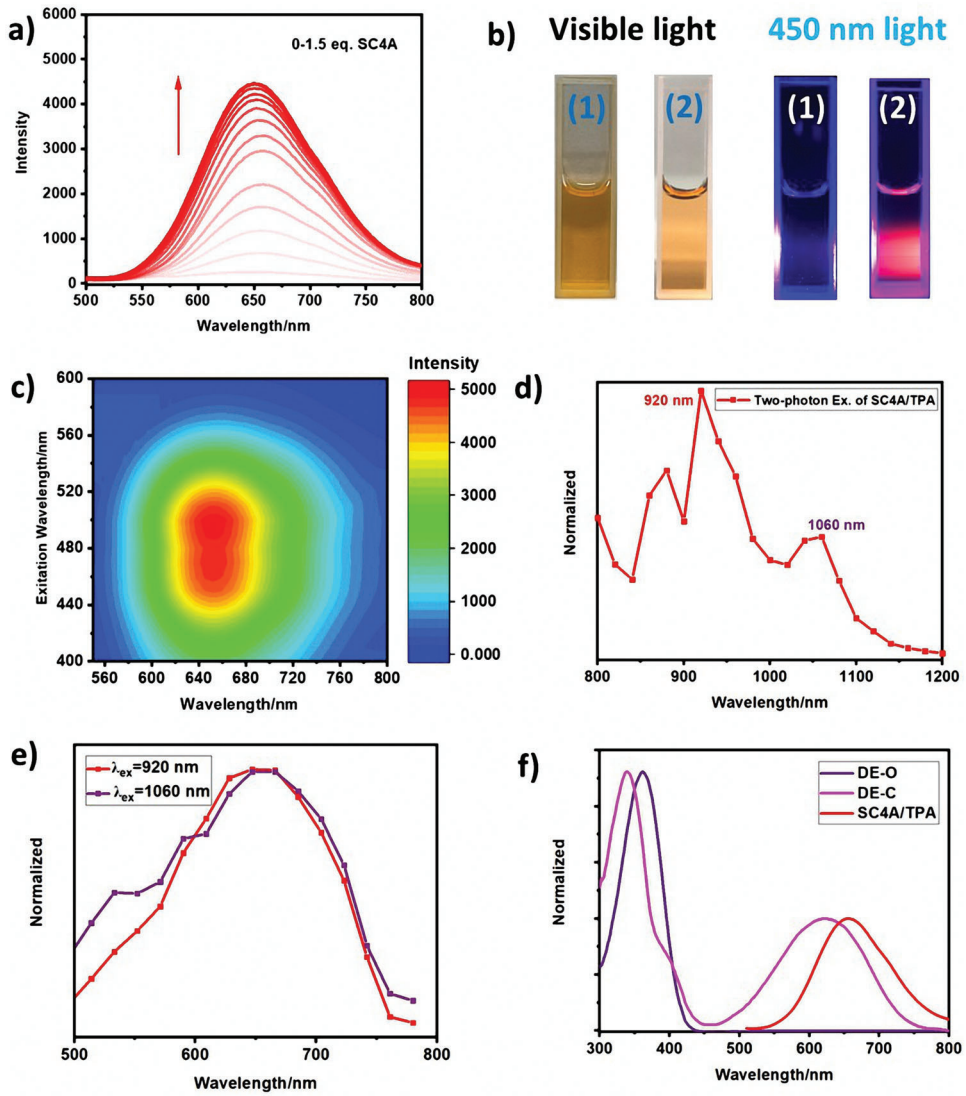

Figure 3. a) Fluorescence spectra of TPA upon addition of different mounts of SC4A (λ_{ex} = 480 nm, 0–1.5 eq.). b) The solution of TPA (1) and SC4A/TPA (2) under visible light (left) or 450 nm light (right), respectively. c) Fluorescence-excitation spectrum of SC4A/TPA. d) Two-photon excited spectrum of SC4A/TPA (λ_{em} = 655 nm). e) Fluorescence spectra of SC4A/TPA under the excitation of NIR light (λ_{ex} = 920 nm, 1060 nm). f) Normalized UV–vis spectra of DE-O, DE-C, and fluorescence spectrum of SC4A/TPA ([SC4A] = [TPA] = [DE-O] = [DE-C] = 10 μM).

efficiently enhanced and gave a strong luminescence signal at 655 nm in the presence of SC4A. Furthermore, the quantum yield of TPA was enhanced from 0.17% to 2.16% by the confinement of SC4A. Figure 3b clearly shows that the solution of TPA alone exhibited relatively weak luminescence. In sharp contrast with TPA, the supramolecular assembly of SC4A/TPA gave bright red color under the 450 nm lamp, which further confirmed that SC4A could confine TPA to give efficient red fluorescence emission. We also studied the influence of different wavelengths of excitation light on the NIR emission of the system. Figure 3c demonstrates that SC4A/TPA could be excited by visible light (440–520 nm) to give efficient fluorescence emission. The assembly with visible light excitation advantages could effectively avoid the shortcomings caused by ultraviolet light excitation, showing broad application prospects in cell imaging. Subsequently, the sulfonatocalix[4]arene without alkyl chain (SC4A-1) and sulfonated β-cyclodextrin (SCD) were also applied to study the confinement effect of negatively charged macrocyclic hosts on the luminescence behavior of TPA. As can be seen from Figures S14 and S15 (Supporting Information), after the addition of SC4A-1 or SCD, the fluorescence intensity of TPA at 655 nm was also increased by 14.0 and 11.2 times, respectively, which was inferior to that in the presence of amphiphilic SC4A (19.2 times). These experiments jointly indicated that the amphiphilic SC4A could effectively confine the TPA and enhance the fluorescence emission of guests. The following reasons may account for the unique phenomenon. First, SC4A could bind with TPA via non-covalent interaction, reducing energy dissipation caused by vibration, rotation, and twisting of excited guests and then benefiting the fluorescence emission of the confined guests.[23] On the other hand,

the amphiphilic SC4A possesses hydrophobic alkyl chains, which could assemble to form stable and ordered nanostructures by the SC4A/TPA complexes, thus reducing the collision of solvent molecules and further benefiting the luminescence of TPA. The guest TPA in the multivalent assembly has a triphenylamine core (donor) and pyridine salt (acceptor) conjugated structure, which is not only beneficial to the extension of absorption and emission wavelength of the luminophores but also may have the property of two-photon absorption.[24] It is exciting that the obtained SC4A/TPA exhibits multiple NIR absorption bands in the wavelength range of 800–1200 nm (Figure 3d). Furthermore, the multivalent assembly of SC4A/TPA was excited by NIR-I (920 nm) and NIR-II (1060 nm) light to give NIR fluorescence signal at 655 nm (Figure 3e). Therefore, the red luminescent multivalent assembly of SC4A/TPA featured the NIR and visible light excited properties, which could avoid the disadvantages caused by ultraviolet excitation and was suitable for cell imaging.

Amphiphilic SC4A not only could enhance the NIR luminescence of TPA by non-covalent interaction and assemble confinement but also assembled with guest to form stable supramolecular nanoparticles, which was conducive to load stimulus-responsive units to construct functional materials. Among many stimulus-responsive methods, photo-regulation has the advantages of simple operation, cleanness, non-pollution, high efficiency, and minimum interference to the system. To this end, the multivalent supramolecular assembly of SC4A/TPA provides a good platform for constructing light-controllable luminescence assembly. Dicationic diarylethene derivative (DE)[25] was selected as the photo-switch unit, which exhibited good reversible photoisomerization performance (Figure S16, Supporting Information) and could co-assemble with the SC4A/TPA to form the photo-stimulus supramolecular assembly. First, we investigated the absorption band of DE to evaluate the potential of which acts as a switch of the NIR emitting system. As shown in Figure 3f, the maximum absorption peak of DE with ring-opened form (DE-O) was 365 nm. Thus the 365 nm light source was selected and applied in the photo-isomerization experiments. After 365 nm light irradiation, the DE-O was changed to the ring-closed pattern (DE-C), and the maximum absorption peak was redshifted to 625 nm. The absorption spectrum of DE-C had a good overlap with the emission signal of NIR luminophore in the wavelength range of 550–750 nm, indicating the excited energy may transfer from TPA to DE-C. Furthermore, the two isomers (DE-O and DE-C) of the selected photo-switch unit showed a weak absorption signal at 450–500 nm; thus, this multivalent assembly was effectively excited by visible light (λ_{ex} = 480 nm) to give NIR luminescence, avoiding the influence of reabsorption. After being irradiated by ultraviolet light (365 nm), the emission peak of the SC4A/TPA/DE-O at 655 nm was gradually decreased (**Figure 4**a), indicating that the energy was transferred from the excited TPA to DE-C in this system. According to the fluorescence intensity change of this multivalent supramolecular assembly at 655 nm, the energy transfer efficiency was calculated to be 83%. In addition, the energy transfer efficiency of SC4A/TPA/DE-O with different ratios of TPA/DE-O was also investigated and gave the best performance of the photo-switch at a 1:1 ratio of TPA/DE-O (Figure S17, Supporting Information). Furthermore, the fluorescence lifetime of SC4A/TPA was decreased from 1.40 to 0.62 ns in the presence of energy acceptor DE-C (Figure S18, Supporting Information), indicating the energy transfer from TPA to the photo-switch DE-C in the co-assembly may go through the Förster mechanism.[26] On the other hand, the maximum absorption peak of DE-C is located at 625 nm, thus the closed form of DE can be photo-isomerized to DE-O under visible light irradiation (>600 nm), avoiding the excitation of TPA. As shown in Figure 4b, the NIR luminescence of the multivalent assembly was recovered after being irradiated by visible light (>600 nm) for 200 s, which may ascribe to the DE-C being isomerized to DE-O, resulting in the energy could not transfer from excited TPA to DE-O in this system. Figure 4c shows that the multivalent supramolecular assembly of SC4A/TPA/DE-O gave bright red light under 450 nm lamp (left). After 365 nm UV light irradiation, the system exhibited negligible red light (Figure 4c, right) under 450 nm light, while the red luminescence of the solution was further recovered after visible light irradiation (>600 nm). Upon alternating 365 nm and visible light irradiation (Figure 4d), the photo-switch process of NIR fluorescence emission could repeat five cycles with slight red luminescence fatigue, indicating this multivalent system based on amphiphilic calix[4]arene could act as reversible photo-controlled NIR luminescent material. Additionally, the fluorescence intensity of the SC4A/TPA/DE-C and SC4A/TPA/DE-O at 655 nm without obvious change under continuous 365 and 600 nm light irradiation, respectively, exhibited good photostability (Figure S19, Supporting Information). Based on the above experiment results, we present the possible mechanism of phot-controllable NIR luminescence (Figure 4e); that is, the ring-opened photo-switch molecule has a higher singlet excited state than the donor (TPA) and cannot act as the energy acceptor and thus displaying NIR luminescence from TPA. After ultraviolet light irradiation, the formed ring-closed DE-C has a lower singlet excited state, which benefits the energy transfer from the singlet TPA to the DE-C, leading to the quenching of red luminescence. In addition, the co-assembly of SC4A/TPA/DE-O showed photo-responsive NIR luminescence under the excitation of NIR light (λ_{ex} = 920 nm, Figure 4f), indicating which could act as a two-photon switch.

Considering the fabricated supramolecular assembly has good NIR luminescence and exhibits photo-controllable performance, we explore its possible application in cell imaging. First, we investigated the cytotoxicity of the SC4A/TPA/DE-O in vitro cell test. Figure S20 (Supporting Information) showed that the survival rate of the cell gave a significant difference ($^*p < 0.05$) after incubated with different concentrations of the SC4A/TPA/DE-O (8–14 μM), manifesting the nanoprobe has weak cytotoxicity compared with the blank group. However, the cell survival rate still reaches 93.5% when the concentration of the NIR probe is at 14 μM, indicating the assembly has good biocompatibility and is suitable for cell imaging. As shown in Figure S21 (Supporting Information), the TPA alone incubated with HeLa cells after 12 h, no obvious fluorescence signal was observed in the confocal imaging experiment, indicating unconfined guest could not act as a satisfactory biological fluorescent probe. In sharp contrast with the TPA, the assembly of SC4A/TPA/DE-O showed red luminescence in the cell imaging experiment (**Figure 5**b). We further studied the ability of SC4A/TPA/DE-O to label the organelles in cancer cells selectively. As can be seen from Figure 5c, the red supramolecular assembly and green mitochondria tracker well coincided, giving yellow lumi-

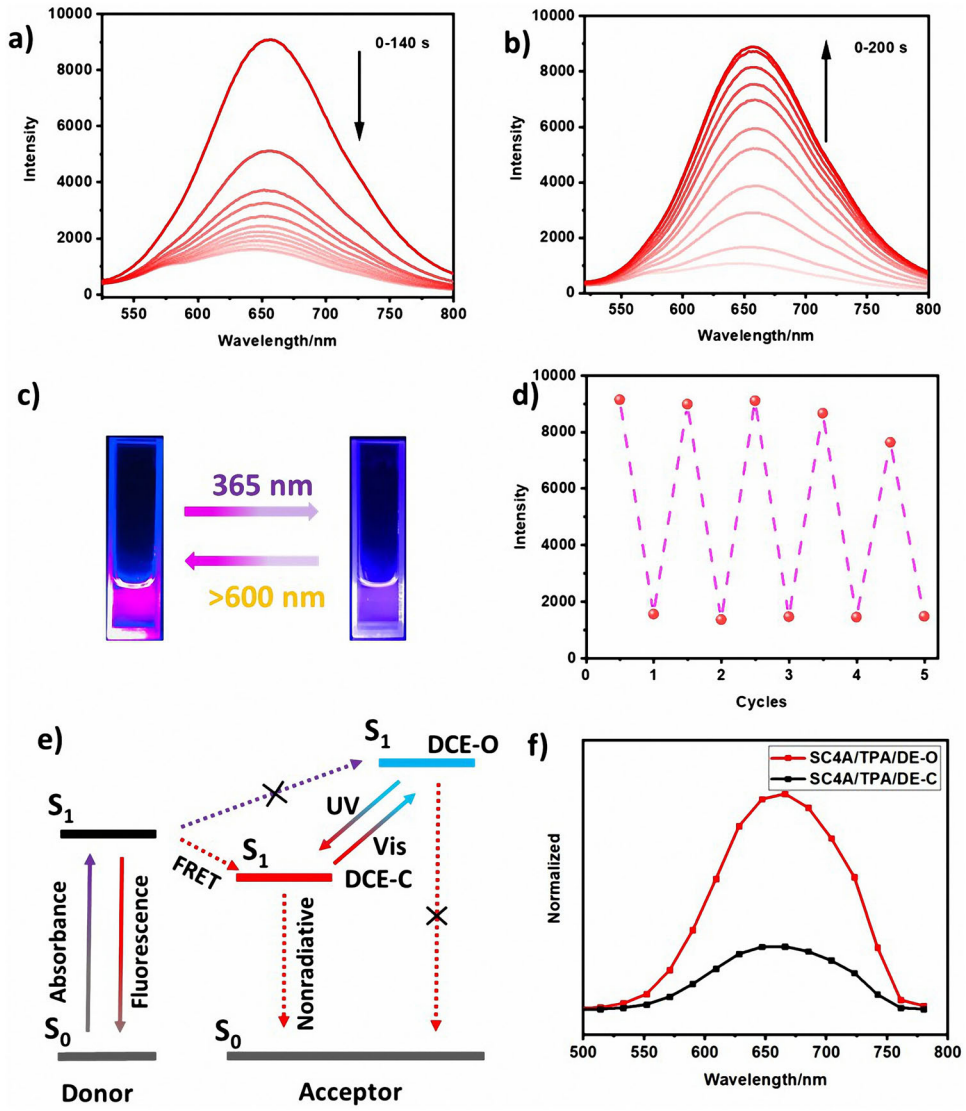

Figure 4. a) Fluorescence spectra of SC4A/TPA/DE-O under 365 nm light irradiation (0–140 s, $\lambda_{ex} = 480$ nm). b) Fluorescence spectra of SC4A/TPA/DE-C under visible light (>600 nm) irradiation (0–200 s, $\lambda_{ex} = 480$ nm). c) The solution of SC4A/TPA/DE-O (left) and SC4A/TPA/ DE-C (right) under visible light (450 nm). d) The luminescence intensity of the system at 655 nm under alternating light irradiation (365 or >600 nm). e) The simplified Jablonski diagram for the illustration of the photo-controllable NIR luminescence mechanism. f) The normalized fluorescence spectra of SC4A/TPA/DE-O and SC4A/TPA/DE-C at 655 nm under the excitation of NIR light ($\lambda_{ex} = 920$ nm) ([SC4A] = [TPA] = [DE-O] = [DE-C] = 10 μM).

nescence sites, and the colocalization coefficient was high up to 0.83 (Figure S22, Supporting Information), indicating the obtained NIR supramolecular assembly could label mitochondria. Zeta potential data showed that the SC4A/TPA/DE-O possesses positive charges on their surface (Figure S23, Supporting Information), leading to their easy entry into mitochondria with intrinsic negative membrane potential. Furthermore, no red luminescence from the assembly was observed in the nucleus (Figure 5d), implying the fabricated assembly was difficult entry the nucleus. We also treated HeLa cells with the lysosomal marker and SC4A/TPA/DE-O, Figure S24 (Supporting Information) gave rare yellow luminescence sites, and the measured colocalization coefficient was 0.28, manifesting the lysosomal marker and supramolecular assembly was not well co-localized in lysosomes. These cell experiments showed that the NIR fluorescent assembly based on the assemble-confinement of amphiphilic SC4A was successfully applied in targeted mitochondrial imaging. Finally, we further investigated the photo-controlled imaging ability of SC4A/TPA /DE-O in cells. Compared with the cells treated with SC4A/TPA/DE-O (Figure 5b–e), negligible red luminescence from the SC4A/TPA/DE-C (Figure 5g; Figure S25, Supporting Information) was observed under the excitation of 450 or 920 nm light respectively, indicating efficient energy transferred from TPA to DE-C, resulting in the quenching of NIR luminescence in cells. Therefore, the two-photon excited light switch based on multivalent supramolecular co-assembly shows wide application in NIR cell imaging and luminescent materials.

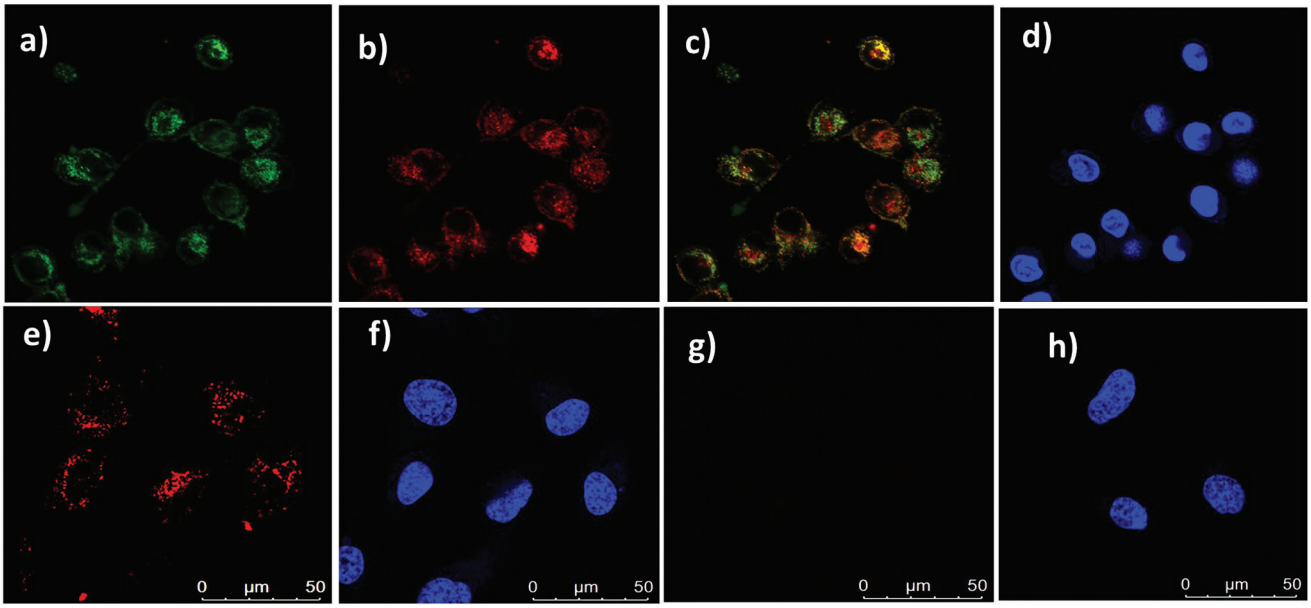

Figure 5. Laser scanning confocal microscopy image of HeLa cells treated with a) Mito-tracker (λ_{ex} = 458 nm). b) SC4A/TPA/DE-O (λ_{ex} = 488 nm). c) Merged (a) and (b). d) Hochest 33 342 (λex = 405 nm). e) SC4A/TPA/DE-O (λex = 920 nm, laser power: 25 mW). f) Hochest 33 342 (λex = 405 nm). g) SC4A/TPA/DE-C (λex = 920 nm, laser power: 25 mW). h) Hochest 33 342 (λex = 405 nm) ([Hochest 33 342] = [Mito-tracker] = [SC4A] = [TPA] = [DE-O] = 10 μm).

3. Conclusion

In conclusion, a light controllable two-photon NIR fluorescent supramolecular assembly was successfully fabricated by the multivalent assembly of amphiphilic sulfonated calixarene, tricationic triphenylamine, and diarylethene derivatives. By the assemble-confinement of SC4A, the weak emission guest-TPA was induced to form nanoparticles with strong NIR luminescence at 655 nm under the excitation of visible and NIR light, along with the efficient enhancement of fluorescence up to 19.2 times. Furthermore, the obtained multivalent supramolecular system could co-assemble with the photo-switch unit, leading to efficient energy transfer from excited TPA to the ring-closed photo-switch after 365 nm irradiation and showing energy transfer efficiency up to 83%, realizing photo-controllable NIR emission in aqueous solution. Finally, the NIR luminescence multivalent supramolecular assembly was successfully applied in mitochondrial localization in HeLa cells and exhibited the ability of photo-controlled two-photon NIR luminescence cell imaging.

Supporting Information

Supporting Information is available from the Wiley Online Library or from the author.

Acknowledgements

J.Y. and J.N. contributed equally to this work. The authors thank the National Natural Science Foundation of China (22201142 and 22131008) and the Haihe Laboratory of Sustainable Chemical Transformations for financial support. The (two-photon) image acquisition was supported by Jing Wu, Biological Imaging and Analysis Laboratory, Medical and Health Analysis Center, Peking University.

Conflict of Interest

The authors declare no conflict of interest.

Data Availability Statement

The data that support the findings of this study are available from the corresponding author upon reasonable request.

Keywords

calix[4]arene, energy transfer, light-controllable, near-infrared fluorescence, supramolecular assembly

Received: June 20, 2023
Revised: August 10, 2023
Published online:

[1] a) Z.-X. Liu, Y. Liu, *Chem. Soc. Rev.* **2022**, *51*, 4786; b) Y. Tang, H. K. Bisoyi, X.-M. Chen, Z. Liu, X. Chen, S. Zhang, Q. Li, *Adv. Mater.* **2023**, *35*, 2300232; c) Y. Tang, X. Wang, G. Zhu, Z. Liu, X.-M. Chen, H. K. Bisoyi, X. Chen, X. Chen, Y. Xu, J. Li, Q. Li, *Small* **2023**, *19*, 2205440.
[2] a) Y. Lee, N. K. Devaraj, *Chem. Sci.* **2021**, *12*, 1090; b) X. Wang, Y. Tang, Y. Qin, P. Zhang, D.-D. Zhang, K. Xue, Y. Cao, Z. Qi, *Chem. Eng. J.* **2022**, *448*, 137632.
[3] M. Votava, B. J. Ravoo, *Chem. Soc. Rev.* **2021**, *50*, 10009.
[4] X. Chen, H. K. Bisoyi, X.-F. Chen, X.-M. Chen, S. Zhang, Y. Tang, G. Zhu, H. Yang, Q. Li, *Matter* **2022**, *5*, 3883.
[5] Z. Wang, C. Sun, K. Yang, X. Chen, R. Wang, *Angew. Chem., Int. Ed.* **2022**, *61*, e202206763.
[6] Z. Zheng, H. Yu, W.-C. Geng, X.-Y. Hu, Y.-Y. Wang, Z.-Z. Li, Y. Wang, D.-S. Guo, *Nat. Commun.* **2019**, *10*, 5762.

[7] H.-T. Feng, Y. Li, X. Duan, X. Wang, C. Qi, J. W Y. Lam, D. Ding, B. Z. Tang, *J. Am. Chem. Soc.* **2020**, *142*, 15966.
[8] M. Lee, S.-J. Lee, L.-H. Jiang, *J. Am. Chem. Soc.* **2004**, *126*, 12724.
[9] R. V. Rodik, S. O. Cherenok, V. Y. Postupalenko, S. Oncul, V. Brusianska, P. Borysko, V. I. Kalchenko, Y. Mely, A. S. Klymchenko, *J. Colloid Interface Sci.* **2022**, *624*, 270.
[10] R. Kumar, A. Sharma, H. Singh, P. Suating, H. S. Kim, K. Sunwoo, I. Shim, B. C. Gibb, J. S. Kim, *Chem. Rev.* **2019**, *119*, 9657.
[11] M. A. Beatty, J. Borges-González, N. J. Sinclair, A. T. Pye, F. Hof, *J. Am. Chem. Soc.* **2018**, *140*, 3500.
[12] H. J. Kim, M. H. Lee, L. Mutihac, J. Vicens, J. S. Kim, *Chem. Soc. Rev.* **2012**, *41*, 1173.
[13] J.-J. Li, Y. Hu, B. Hu, W. Wang, H. Xu, X.-Y. Hu, F. Ding, H.-B. Li, K.-R. Wang, X. Zhang, D.-S. Guo, *Nat. Commun.* **2022**, *13*, 6279.
[14] S. Fernández-Abad, M. Pessêgo, N. Basílio, L. García-Río, *Chem. - Eur. J.* **2016**, *22*, 6466.
[15] I. Shulov, R. V. Rodik, Y. Arntz, A. Reisch, V. I. Kalchenko, A. S. Klymchenko, *Angew. Chem., Int. Ed.* **2016**, *55*, 15884.
[16] F. Rodler, B. Schade, C. M. Jäger, S. Backes, F. Hampel, C. Böttcher, T. Clark, A. Hirsch, *J. Am. Chem. Soc.* **2015**, *137*, 3308.
[17] M. Huo, X.-Y. Dai, Y. Liu, *Angew. Chem., Int. Ed.* **2021**, *60*, 27171.
[18] a) L. Ma, Q. Xu, S. Sun, B. Ding, Z. Huang, X. Ma, H. Tian, *Angew. Chem., Int. Ed.* **2022**, *61*, e202115748; b) Y. Fu, X. Zhang, J. Liu, G. Qian, Z. P. Xu, R. Zhang, *J. Mater. Chem. B* **2022**, *10*, 3366; c) X. Zhang, Y. Fu, J. Liu, G. Qian, J. Zhang, R. Zhang, Z. P. Xu, *Nanoscale* **2020**, *12*, 22527.
[19] H.-J. Yu, Q. Zhou, X. Dai, F.-F. Shen, Y.-M. Zhang, X. Xu, Y. Liu, *J. Am. Chem. Soc.* **2021**, *143*, 13887.
[20] a) H.-Y. Jung, B. Kim, M. H. Jeon, Y. Kim, *Samll* **2022**, *18*, 2103523; b) D. Kim, A. Aktalay, N. Jensen, K. Uno, M. L. Bossi, V. N. Belov, S. W. Hell, *J. Am. Chem. Soc.* **2022**, *144*, 14235.
[21] Y.-X. Wang, Y.-M. Zhang, Y. Liu, *J. Am. Chem. Soc.* **2015**, *137*, 4543.
[22] a) J. Yu, Y.-H. Zhang, F.-L. Chen, S.-S. Xiao, L. Li, *Dyes Pigm.* **2020**, *183*, 108748. (b) X.-M. Chen, Q. Cao, H. K. Bisoyi, M. Wang, H. Yang, Q. Li, *Angew. Chem., Int. Ed.* **2020**, *59*, 10493.
[23] X.-K. Ma, Y. Liu, *Acc. Chem. Res.* **2021**, *54*, 3403.
[24] A. Bhaskar, G. Ramakrishna, Z. Lu, R. Twieg, J. M. Hales, D. J. Hagan, E. V. Stryland, T. Goodson, *J. Am. Chem. Soc.* **2006**, *128*, 11840.
[25] C.-H. Wang, Y. Liu, *Mater Today Chem* **2022**, *25*, 100954.
[26] J. Yu, H. Wang, X.-Y. Dai, J. Niu, Y. Liu, *Chem. Commun.* **2023**, *59*, 1457.